HHS Public Access

Author manuscript

Dev Biol. Author manuscript; available in PMC 2017 December 13.

Published in final edited form as:

Dev Biol. 2014 August 15; 392(2): 221–232. doi:10.1016/j.ydbio.2014.05.024.

Cdc42 is required in a genetically distinct subset of cardiac cells during *Drosophila* dorsal vessel closure

David Swope[1], **Joseph Kramer**[1], **Tiffany R. King**[1,2], **Yi-Shan Cheng**[1], and **Sunita G. Kramer**[1,2,*]

[1]Department of Pathology and Laboratory Medicine, Rutgers-Robert Wood Johnson Medical School, 675 Hoes Lane Piscataway, NJ 08854, Phone: (732) 235-4226, Fax: (732) 235-4825

[2]Graduate Program in Cell and Developmental Biology, Rutgers Graduate School of Biomedical Sciences at Robert Wood Johnson Medical School, 675 Hoes Lane Piscataway, NJ 08854

Abstract

The embryonic heart tube is formed by the migration and subsequent midline convergence of two bilateral heart fields. In *Drosophila* the heart fields are organized into two rows of cardioblasts (CBs). While morphogenesis of the dorsal ectoderm, which lies directly above the *Drosophila* dorsal vessel (DV), has been extensively characterized, the migration and concomitant fundamental factors facilitating DV formation remain poorly understood. Here we provide evidence that DV closure occurs at multiple independent points along the A-P axis of the embryo in a “buttoning” pattern, divergent from the zippering mechanism observed in the overlying epidermis during dorsal closure. Moreover, we demonstrate that a genetically distinct subset of CBs is programmed to make initial contact with the opposing row. To elucidate the cellular mechanisms underlying this process, we examined the role of Rho GTPases during cardiac migration using inhibitory and overexpression approaches. We found that Cdc42 shows striking cell-type specificity during DV formation. Disruption of Cdc42 function specifically prevents CBs that express the homeobox gene *tinman* from completing their dorsal migration, resulting in a failure to make connections with their partnering CBs. Conversely, neighboring CBs that express the orphan nuclear receptor, *seven-up*, are not sensitive to Cdc42 inhibition. Furthermore, this phenotype was specific to Cdc42 and was not observed upon perturbation of Rac or Rho function. Together with the observation that DV closure occurs through the initial contralateral pairing of *tinman-expressing* CBs, our studies suggest that the distinct buttoning mechanism we propose for DV closure is elaborated through signaling pathways regulating Cdc42 activity in this cell type.

Keywords

Drosophila; Dorsal vessel; Rho GTPase; Cdc42

[*]**Author for Correspondence**: Rutgers, Robert Wood Johnson Medical School, Department of Pathology and Laboratory Medicine, kramersg@rwjms.rutgers.edu.

INTRODUCTION

Cardiogenesis requires a precise series of morphogenetic movements in order to create the three-dimensional structure of the heart. One of the earliest sets of movements involves the bilateral and synchronized migration of groups of cardiomyocytes towards the midline of the embryo where they converge to form the linear heart tube, a process called cardiac fusion (Abu-Issa and Kirby, 2007). Defects in cardiac fusion results in the cardia bifidia phenotype, which is defined by the presence of two separated hearts, due to a failure of the two cardiac fields to converge into a single heart tube. The ability to easily identify this phenotype has uncovered crucial genes that are required for cardiac migration (Kawahara et al., 2009; Totong et al., 2011; Trinh and Stainier, 2004). However the cellular mechanisms that facilitate directed cardiac migration as well as cell-cell interactions once cardiac cells approach their destination, remain poorly understood.

Development of the *Drosophila* embryonic heart, or dorsal vessel (DV), which closely resembles the vertebrate heart at its transient linear tube stage, provides an ideal genetic model system to study cardiac fusion due to its simple, yet highly analogous structure (for reviews see (Cripps and Olson, 2002; Medioni et al., 2009; Tao and Schulz, 2007)). During DV development, cardioblasts (CBs) are specified in two bilaterally symmetric rows that collectively migrate to the dorsal midline where they make specific E-Cadherin based adhesive contacts to form a single layer linear tube with a central lumen (Haag et al., 1999; Medioni et al., 2008; Santiago-Martinez et al., 2008). The DV is subdivided into a narrower anterior portion called the aorta and a wider posterior heart proper. The cardioblasts (CBs) can be subdivided into either smaller contractile cells that express the homeobox gene *tinman* (Tin+ CBs), or larger rounded cells expressing the orphan nuclear receptor, *seven-up* (Svp+ CBs) (Gajewski et al., 2000). In the heart, the two cells types are functionally distinct. *Tinman* expression allows CBs to differentiate into muscle cells used for pumping of hemolymph, as opposed to *seven-up* expression, which allows for differentiation into the inflow tracts called ostia (Molina and Cripps, 2001). A unique aspect of DV assembly is that each row of cells consists of exactly 52 CBs that align precisely with their contralateral counterparts to form a functional heart tube. This remarkable level of accuracy allows for a straightforward analysis of the mechanisms underlying cardiac fusion.

One well-known morphogenetic event requiring the regulation of cell migration and cell-cell interaction is *Drosophila* dorsal closure, a paradigm of epithelial fusion that involves the sealing of a hole in the embryo by the joining of two epithelial sheets (for review see (Martin and Wood, 2002)). The cells in the front row, or leading edge cells, project actin-based filopodia that are critical for the zippering together of the two epithelial sheets as well as the cell-cell matching that is required to keep segments aligned across the epithelial seam (Jacinto et al., 2000; Millard and Martin, 2008). Consistent with this idea, mutations that affect actin filopodial dynamics lead to an increase in dorsal closure defects (Gates et al., 2007; Jacinto et al., 2000).

The Rho family of GTPases is a highly-conserved group of proteins shown to modulate a wide variety of cellular processes including cell motility, cell shape changes and cell adhesion by linking receptors at the plasma membrane to the actin cytoskeleton (for reviews

see (Etienne-Manneville and Hall, 2002; Hall, 2012; Johndrow et al., 2004). The most well studied function of Rho GTPases is to control the organization and the dynamics of the actin cytoskeleton by functioning as molecular switches that cycle between active, GTP-bound and inactive GDP-bound states. Once activated, Rho GTPases mediate their effects on the cell through interaction with downstream effector proteins. Key members of this protein family, Rho, Rac and Cdc42 are capable of interacting with a large number of effector proteins, suggesting that they each regulate several distinct signal transduction pathways.

Particularly, members of the Rho family of GTPases have emerged as critical players in epithelial morphogenesis (Van Aelst and Symons, 2002). Genetic analysis has implicated Rho1, Rac1 and Cdc42 in the process of *Drosophila* dorsal closure (Harden et al., 1999). Despite the similarities between these family members, experiments that interfered with the function of Rho1, Rac1 or Cdc42 by expression of dominant negative forms revealed that these proteins play distinct roles during the dorsal closure process. For example, Rac1 is required for the establishment or maintenance of the actomyosin contractile apparatus along the entire leading edge of the dorsal epidermis (Harden et al., 1995), while Rho1 is required for maintaining the integrity of the leading edge cytoskeleton specifically in cells flanking the segment borders (Harden et al., 1999). Cdc42, was shown to have conflicting roles in both establishing and maintaining the leading edge cytoskeleton as well as its down regulation via the serine/theonine kinase DPAK (Harden et al., 1999). Subsequent studies using loss-of-function analysis further confirmed the roles for Rho1, Rac1 and Cdc42 in the dorsal closure process (Abreu-Blanco et al., 2012; Campos et al., 2010; Denholm et al., 2005; Lu and Settleman, 1999; Magie et al., 1999; Wood et al., 2002; Woolner et al., 2005), demonstrating the efficacy of the dominant negative approach for uncovering novel roles for Rho GTPases during development.

Although GTPases have been well studied in the context of epithelial morphogenesis, the role of these family members are not well characterized during embryonic heart development. During *Drosophila* DV formation, as the two rows of CBs migrate to the dorsal midline, they lie in close proximity to the leading edge cells in the dorsal epidermis (DE). Therefore, while the two rows of CBs are undergoing DV closure, the overlying epithelium is simultaneously undergoing dorsal closure. Studies have implicated the type IV collagen-like protein Pericardin in mediating the coordinated movement of the DE and the CBs (Chartier et al., 2002). However, despite the close association of the CBs with the overlying ectoderm, it is not known whether dorsal closure and cardiac fusion occur via similar morphogenetic behaviors and more specifically whether the Rho GTPases play a similar role during these two morphogenetic processes.

In this study we examine the cellular mechanisms underlying *Drosophila* DV closure. Using a live imaging approach, we show that DV closure occures via a “buttoning” mechanism where genetically distinct leader CBs in each row make contact with their contralateral partners across the midline prior to their immediate neighbors. Furthermore, we examine the role of key members of the Rho GTPase family (Rho, Rac and Cdc42) during cardiac fusion, using inhibitory and overexpression approaches. Our studies reveal an important role for Cdc42 in this process. We show that Cdc42 is required specifically in the Tin+ CB leader cells to drive their forward migration to the embryonic midline ahead of their Svp+

neighbors. Loss of Cdc42 activity in the Tin+ CBs results in a failure of this cell type to complete the cardiac fusion process, resulting in holes in the DV, while loss of Cdc42 in the Svp+ CBs has no effect on DV morphogenesis. Furthermore, this phenotype was specific to Cdc42 and was not observed upon perturbation of Rac or Rho function. Thus, our data indicate that genetically distinct cell types of the embryonic heart tube exhibit differential requirements for small Rho GTPase function. Together with the observation that DV closure occurs through the initial contralateral pairing of Tin+ CBs, our studies suggest that the distinct buttoning mechanism we propose for DV closure is elaborated through signaling pathways regulating Cdc42 activity in this cell type.

MATERIALS AND METHODS

Fly stocks and genetics

Fly crosses were preformed at 25°C and maintained o n standard medium. The following stocks were used: *UAS-Rho1*^{WT} (BL#28872), UAS-*Rho1*^{N19} (BL#7328), *UAS-Rac1*^{WT} (BL#28874), *UAS-Rac1*^{N17} (BL#6292), *UAS-Cdc42*^{N17} (BL#6288), *UAS-Cdc42*^{WT} (BL#28873), *UAS-Cdc42*^{V12} (BL#6287), *UAS-Pak-myr* (BL#8804), *69B-GAL4* (BL#1774), *Hand-GAL4* (Han et al., 2006), *UAS-GFP-moe* (Chihara et al., 2003), *Prc*-GAL4 (Chartier et al., 2002), *Svp*-GAL4 (BL#47912), and UAS-*RedStinger* (BL#8545). *Hand*-GFP (Han et al., 2006), *yw*, and *w*^{1118} stocks were used as wild type controls. To visualize actin protrusions in CBs of the living embryo, *Hand-GAL4* was recombined with *UAS-GFP-moe* on the second chromosome.

Immunohistochemistry and confocal microscopy

Embryos were dechorionated and then fixed in 4% formaldehyde in PBS at room temperature and stained according to standard protocols as previously described (Macabenta et al., 2013). The following primary antibodies were used: mouse anti-α-Spectrin [Developmental Studies Hybridoma Bank (DSHB), 1:10], mouse anti-Wingless (DSHB, 1:10), mouse anti-Pericardin (DSHB, 1:10), rabbit anti-β3-tubulin (1:1000, R. Renkawitz-Pohl), and rabbit anti-GFP (1:500, Invitrogen). For secondary antibodies, goat anti-mouse or anti-rabbit conjugated to either Alexa 488 or 555 (1:500; Invitrogen) were used. Fixed and stained embryos were carefully staged using head and gut morphology and mounted on glass cover slips in 60% glycerol. Confocal z-sections were obtained at ambient temperature on an inverted Olympus IX81 with a Crest CARV II confocal unit using a Plan VApo/340 60X/1.20 NA W objective and an ORCA-EM CCD Digital camera (Hamamatsu).

Cross-sections of fixed embryos

Well slides for viewing embryos in cross section were prepared by painting small circles of valve lubricant (Dow Corning) on 24×60 mm^2 rectangular coverslips. A solution of heptane and adhesive tape glue was applied in two layers, allowing the heptane to evaporate between applications. Embryos were carefully staged using head and gut morphology and cut approximately two-thirds of the way from the most anterior end. Embryos were propped up vertically on the center of the well slide and a solution of 60% glycerol diluted in PBS was added drop-wise into the well, such that all embryos were completely immersed. The embryos were then imaged using an Olympus confocal microscope (described above).

Live embryo imaging and measurements

Embryos at approximately stage 15 were collected from agar plates, dechorianated in 50% bleach and placed on a cover slip with a thin layer of valve lubricant (Dow Corning). Embryos were immersed in Halocarbon oil 700 (Sigma) and immediately imaged using an Olympus confocal microscope. Z-sections of developing embryos were collected for 40-120 total minutes in 2-minute intervals. Still frame images were then compiled using the ImageJ software to create movies. CB-CB measurements were performed between contralateral CB nuclei beginning when A5 Svp+ CBs were approximately 25 m apart from each other, to control for staging. 3 sets of measurements were recorded during DV closure for each embryo (WT; n=7) (*Cdc42*^{N17}; n=6). To distinguish between Svp+ CBs and Tin+ CBs we used either *Svp-GAL4*; UAS-*RedStinger* embryos or identified *seven-up* CBs by counting CB number from the posterior end of the embryo as well as distinct *seven-up* nuclear morphology (see Fig. S3). 3 sets of measurements were recorded during DV closure for each embryo (WT n=7; *Cdc42*^{N17} mutants n=6). Filopodial measurements of Control (*yw; Hand-Gal4, UAS-GFP-moe*) and Cdc42 mutant (*Hand-Gal4, UAS-GFP-moe; UAS-Cdc42*^{N17}*)* embryos were preformed using iVision Software. Filopodial length (>1uM) and number were measured from the posterior-most portion of the DV to approximately segment A5 (125uM). 3 series of measurements were conducted from embryos when A5 CBs were 30uM, 20uM and 10 uM apart from their contralateral partner, to control for proper staging. Statistical analysis was done using a Student two-tailed t-test (Control n=3; *Cdc42*^{N17} mutants n=3).

RESULTS

A genetically distinct subset of CBs makes initial contact at the dorsal midline

To investigate the morphogenetic events that occur during *Drosophila* cardiac fusion as compared to dorsal closure in the overlying dorsal epidermis, we used live imaging to track migrating DE cells or CBs labeled with GFP-moe, which localizes to the cortical actin cytoskeleton, providing a strong *in vivo* marker for cell shape and actin dynamics during cell morphogenesis (Chihara et al., 2003; Edwards et al., 1997). As previously shown, dorsal closure occurs via a “zippering” mechanism where a hole between tissues is sealed by the knitting together of the opposing cells from two ends (Jacinto et al., 2000). We replicated these findings by performing time-lapse confocal microscopy on *69B-GAL4; UAS-GFP-moe* embryos. In these embryos, GFP-moe is expressed in all epidermal cells via the *69B-GAL4* driver and strongly localizes to the leading edge of the dorsal epidermis. Figures 1A–D represent images from time lapsed sequences extracted from Movie S1. To investigate the mechanisms underlying cardiac fusion, we performed the same experiment on *Hand-GAL4,UAS-GFP-moe* embryos. *Hand-GAL4* drives strong expression in the DV (Sellin et al., 2006). Figures 1E–H represent images from time lapsed sequences extracted from Movie S2. These experiments revealed that in contrast to epithelial closure, which occurs via a zippering from the anterior and posterior ends of the embryo towards the center (Fig. 1L,M), DV closure occurs at multiple independent points along the anterior-posterior axis via an alternative “buttoning” mechanism (Fig. 1N,O).

Our results show that during DV formation, certain regions along each CB row come together at the dorsal midline in advance of adjacent tissue, resulting in a buttoning pattern of closure. To determine whether initial contact is made by specific subpopulations of CBs, we double-labeled fixed *Hand-GAL4,UAS-GFP-moe* embryos with anti-Wingless (Wg), which labels the six pairs of *Svp*+ CBs in the heart region of the DV (Lo et al., 2002), as well as anti-GFP to label all CBs. By examining embryos at stage 16, we were able to determine that in the heart the *Tin*+ CBs behave as leader cells, making contact with the opposing row before the *Svp*+ CBs (Fig. 1I–K). We scored this phenotype in 72% of the embryos we examined (n=18). Due to this unique behavior, we hypothesized that the *Tin*+ CB function as “pioneers” to guide the cardiac fusion process.

Perturbation of Rho GTPase function affects DV formation

Rho GTPase proteins are critical regulators of the cytoskeleton during the processes of cell migration and outgrowth (Johndrow et al., 2004). Rho, Rac1 and Cdc42 are highly conserved family members and have been shown to play important, but distinct functions during *Drosophila* dorsal closure (Harden et al., 1995; Harden et al., 1999; Jacinto et al., 2000; Magie et al., 1999). However, the role of these proteins during DV closure is unknown. To study the potential role of these Rho GTPases during DV formation, we individually expressed wild type or dominant-negative alleles of Rho1, Rac1 and Cdc42 specifically in the DV using the *Hand-GAL4* driver. The chromosome carrying the *Hand-GAL4* transgene was recombined with the *UAS-GFP-moe* to enable visualization of the cortical actin cytoskeleton. Stage 17 embryos were fixed and stained with anti-αSpectrin to discern CB lateral and luminal membranes as well as anti-GFP to observe the actin cytoskeleton. In this way we could determine whether Rho GTPase expression caused changes to CB polarity and/or DV morphogenesis.

To examine the effects of wild type Rho1 overexpression in the DV, we examined *Hand-GAL4,UAS-GFP-moe; UAS-Rho1^{WT}* embryos for defects in DV formation. Overexpression of Rho1 (Fig. 2D–F) in the DV showed stronger accumulation of αSpectrin at CB lateral membranes (94%; n=17) compared to controls (Fig. 2A–C) suggesting potential CB polarity defects. However in these embryos CBs were able to migrate to the dorsal midline and attach to their contralateral partners (Fig. 2E) (Table 1). Loss of Rho1 function was examined by expression of the dominant-negative form Rho^{N19} (UAS-*Rho1^{N19}*). While we did not observe significant defects in CB cell polarity in *Hand-GAL4,UAS-GFP-moe; UAS-Rho1^{N19}* embryos (Fig. 2G), we did observe the presence of small holes in the DV that were most often observed between the *Svp*+ CBs (Fig. 2G–I) (57%; n=14). These gaps, however, were also observed in the wild type DV at this stage, although to a lesser extent (Table 1). Because these gaps are transient in WT embryos, we hypothesize that the increase in frequency of these gaps in *Hand-GAL4,UAS-GFP-moe; UAS-Rho1^{N19}* embryos could be due to a delay or premature arrest in DV closure. Furthermore, expression of either wild-type Rac1 (*UAS-Rac1^{WT}*) (Fig 2J–L) or dominant negative Rac1 (*UAS-Rac1^{N17}*) (Fig. 2M–O) did not cause significant defects in CB polarity or overall DV defects (Table 1), although we occasionally observed CB mispositioning at certain points along the length of the DV (Fig. 2M).

Finally, we tested the importance of Cdc42 during DV formation. Notably, expression of the dominant negative form of Cdc42 (*UAS-Cdc42^{N17}*) resulted in a unique DV phenotype (Fig. 3D–F) not observed in other Rho GTPase mutants (Fig. 2). Specifically in *Hand-GAL4,UAS-GFP-moe; UAS-Cdc42^{N17}*embryos, we observed the presence of large holes along the length of the DV, which could be clearly seen with anti-GFP labeling (Fig. 3E). In these regions, opposing CBs failed to make contact. We observed this defect in 82% of embryos (n=45) and this phenotype was never observed in wild type (Fig. 3B). Importantly, dorsal closure occurred normally in these embryos (Fig. 3I) indicating that the defects we observed were not due indirectly to the failure of the embryo to complete embryogenesis or the dorsal closure process.

Interestingly, the large holes seen in *Cdc42^{N17}*-expressing embryos were predominantly localized to the heart region of the DV, which resides in segments A5-A8. In the aorta region of embryos that expressed *Cdc42^{N17}*, we observed defects in CB-CB contact at a much lower level than in the heart region (13% (n=45) compared to the 82% we observed in the heart), although we did frequently observe defects in CB morphology in the aorta (93%, n=14) (Fig. 3H). Furthermore, although we were unable to ascertain whether the CBs in the heart region had defects in CB polarity due to the severe disruption of the DV (Fig. 3D), αSpectrin staining in the aorta revealed no significant polarity defects (Fig. 3H).

It is possible that the CB contact defects seen in *Cdc42^{N17}* expressing embryos were a consequence of overexpression and not interference of downstream *Cdc42* targets; therefore we examined the effects of expressing a wild type form of *Cdc42* in the DV. Unlike embryos expressing *Cdc42^{N17}*, we did not observe the presence of large holes in the heart region of the DV in *Hand-GAL4,UAS-GFP-moe; UAS-Cdc42^{WT}* embryos (0%; 0/23) (Fig. 3K), although minor gaps appeared to persist specifically between ostia cells (arrow) (35%; 8/23), consistent with *Rho1^{N19}* mutants (Fig. 2G). Moreover, the aortas of *Hand-GAL4,UAS-GFP-moe; UAS-Cdc42^{WT}* embryos (Fig. 3J) were indistinguishable from wild type (*w^{1118}*) (Fig. 3G). Furthermore, expression of constitutively active *Cdc42* (*UAS-Cdc42^{V12}*) did not produce cell contact abnormalities (Fig.S1), as seen in *Cdc42^{N17}* expressing embryos (Fig. 3E), although in most embryos, we did observe minor defects in CB morphology and polarity (92%; 11/12). Together, our results show that interference with Cdc42 activity through expression of a dominant negative form of the protein in the DV produces distinctive and substantial defects in DV morphogenesis.

During their dorsal migration, the CBs are flanked by non-contractile pericardial cells (PCs) (Ruggendorff et al.,1994) that are loosely associated with CBs and have been shown to function post embryonically as nephrocytes (Crossley, 1972) and contribute to the adult wing heart (Togel et al., 2008). The complete function of PCs during DV closure still remains unclear, although studies have shown that they secrete the type IV collagen-like protein Pericardin, which has been implicated in mediating the coordinated movement of the DE and the CBs (Chartier et al., 2002). In order to examine whether the PCs also require Cdc42 activity, we expressed dominant negative *Cdc42^{N17}* in all PCs using the *Prc-GAL4* driver. We observed no change in Pericardin staining (Fig. S2B) or DV formation (Fig. S2D) in *UAS-Cdc42^{N17}; Prc-GAL4* embryos. Additionally, when Cdc42 activity is inhibited in the CBs in *Hand-GAL4,UAS-GFP-moe;UAS-Cdc42^{N17}* embryos, Pericardin staining

surrounding the CBs is maintained (Fig. S2E–G). Taken together, these results indicate that *Cdc42* is essential specifically in the CBs for mediating proper DV closure.

Dominant-negative *Cdc42* expression causes diminished protrusions and perturbed cell migration in specific areas of the DV

Because expression of dominant negative *Cdc42* caused such a distinct and compelling cardiac phenotype, we decided to further characterize the DV in these embryos. We first performed live imaging analysis on *Hand-GAL4,UAS-GFP-moe* embryos to view actin dynamics in wild type embryos. During normal morphogenesis of the DV, CBs extend actin protrusions towards the embryonic midline as they migrate to the midline and converge with their contralateral partners (Fig. 4 A-D, Movie S3). Because Cdc42 has been implicated in mediating actin based cell protrusion during cell migration in other tissues (Abreu-Blanco et al., 2012; Jacinto et al., 2000; Nobes and Hall, 1995; Wood et al., 2002), we were interested in determining whether the large holes in the DV that we observed in $Cdc42^{N17}$ expressing embryos could be due to reduced CB protrusion length and migration. It is also feasible that these large holes were caused by a failure of contralateral CBs to properly adhere to each other once they made initial contact, as Rho GTPases have been also shown to affect levels of E-cadherin and adherens junction formation (Eaton et al., 1995; Fox et al., 2005; Pirraglia et al., 2006; Warner and Longmore, 2009). To test this hypothesis, we also performed live imaging analysis on $Cdc42^{N17}$ expressing embryos. Still frames taken from time-lapse movies (Movie S4) of *Hand-GAL4,UAS-GFP-moe; UAS-*$Cdc42^{N17}$ embryos show distinct areas along the length of each CB row that have reduced filopodial protrusion number [21.7 M±4.2 (Figs. 4E–H)] as compared to wild type [30.1 M±8.9, $P<0.05$ (Figs. 4A–D, Movie S3)]. Moreover, as seen in Movie S4, the cells that have reduced filopodial protrusions also appear to have reduced migratory behavior. These small stretches of CBs do not reach the dorsal midline and thus fail to make contact with their contralateral partners, accounting for the holes we observed in fixed embryos (Figs. 3D–F). Moreover, these holes in the DV fail to close even in larval stages (data not shown), ruling out that the CBs are delayed in reaching the dorsal midline. Together, these data show that *Cdc42* governs cell motility and actin protrusions in a subset of CBs in the developing DV. Also, it is important to note that we did not observe a complete failure of specific CBs to migrate to the midline. Rather, we observed that the two rows of CBs were able to migrate from their lateral-most positions in stage 13 embryos to the dorsal region of the embryo. However, upon approaching the dorsal midline, this forward migration was disrupted in a subset of CBs.

Tin+ CB pioneers are hindered following $Cdc42^{N17}$ expression

The DV can be subdivided into two genetically and morphologically distinct sets of CBs. CBs that express the homeodomain gene *tinman* (Tin+) are cubioidal in shape, while the CBs expressing the orphan nuclear receptor *seven-up* (Svp+) are more elongated. In the heart, three doublets of *seven-up* CBs further differentiate into ostia cells, functioning as inflow tracts of the heart in late stage embryonic development (Lo et al., 2002; Molina and Cripps, 2001). Our results show that DV closure occurs via a “buttoning” mechanism where specific CB leader cells along the length of each row, make initial contact across the midline (Fig. 1E–H). Moreover, we have identified these CB pioneer cells as the *Tin+* CBs (Fig. 1I–K). Due to the periodic pattern of the holes we observed in embryos expressing dominant

negative Cdc42 (Fig. 3E), we hypothesized that a specific CB subtype fails to make contact in these embryos. To determine the identity of these CBs, we double stained early stage 16 wild type and *Hand-GAL4,UAS-GFP-moe;UAS-Cdc42^{N17}* embryos with GFP to label the DV, and anti-Wingless (Wg) to mark the *Svp+* CBs in the heart. In addition to labeling Svp+ CBs, we also marked Tin+ CBs in the DV with anti-β3-tubulin and cell membranes with anti-αSpectrin. As seen previously (Fig. 1I–K), the Tin+ CBs come into contact at the midline prior to the *Svp+* CBs in wild type embryos (Fig. 5A–F). In contrast, in embryos expressing *Cdc42^{N17}*, the areas of contact are limited to the Svp+ CBs and the Tin+ CBs fail to make contact with their contralateral partners (Fig. 5G–L). Furthermore, staining with anti-Wg (Fig. 5 G,I) and anti β3-tubulin (Fig. 5K,L) also demonstrated that the defects we observed in *Hand-GAL4,UAS-GFP-moe;UAS-Cdc42^{N17}* embryos were not due to a loss of either the Svp+ or Tin+ CB cell type.

Our findings thus far suggest that loss of Cdc42 activity specifically affects the Tin+ CBs. To further test this idea, we drove expression of *Cdc42^{N17}* specifically in the Svp+ CBs. In these embryos, loss of Cdc42 activity did not cause any significant phenotypes in either the heart (Fig. 3L, Table 1) or the aorta (data not shown). Moreover, overexpression of the activated form of Cdc42 (*Cdc42^{V12}*) specifically in the Svp+ CBs also did not cause any significant defects (Fig. S1 G-I). Together these data strongly support a model in which Cdc42 is specifically required for the migration of Tin+ CBs during DV closure.

To better characterize the differences between wild type and *Cdc42^{N17}* embryos, we wanted to obtain measurements that reflected the distances between contralateral CBs along the entire length heart section of the DV, which spans from segments A5-A8. Because it was difficult to clearly discern cell boundaries using the GFP-moe reporter, we decided to measure the relative distances between CB nuclei. We used embryos carrying the *Hand-GFP* transgene, which constitutively labels the nuclei of CBs (and a subset of pericardial cells) with GFP as well as a copy of *Svp-GAL4* and *UAS-RedStinger* (Posakony et al., 2004) to specifically label the Svp+ CBs in wild type embryos. In these embryos, Svp+ CB nuclei (red) can be distinguished from Tin+ CBs green (Fig. 6A). Measurements were taken between contralateral CBs nuclei in segments A5-A8 beginning when A5 Svp+ CBs were approximately 25 m apart from each other, to control for staging. Figure 6C and D show that the distance between Tin+ CBs is significantly smaller than the distance between Svp+ CBs in segments A5-A7 of the heart. These results are consistent with our findings that the Tin+ CBs make contact across the midline prior to the Svp+ CBs (Fig. 1I–K). In *Hand-GFP* embryos expressing *Cdc42^{N17}* with *Hand-GAL4*, we were unable to use *UAS-RedStinger* to specifically label Svp+ CBs. In these embryos, we were able to reliably identify Svp+ CBs both by counting the nuclei from the posterior end as well as size, shape and GFP staining intensity (Fig. 6B; see also Materials and Methods and Fig. S3). Strikingly, in *Cdc42^{N17}* expressing embryos, we see that the Tin+ CBs are now significantly further apart than the Svp+ CBs (Fig. 6C–D). Thus, Tin+ CBs, which normally serve as pioneer cells during morphogenesis, display defects in migration when expressing mutant *Cdc42*.

Loss of Cdc42 activity does not interfere with Svp+ CB morphogenesis

Following CB migration to the midline, the CBs undergo dynamic cell shape changes and make E-cadherin based attachments with their contralateral partners at dorsal and ventral sites while remaining unattached in between (Haag et al., 1999; Medioni et al., 2008; Santiago-Martinez et al., 2008). In this way a lumen is formed along the length of the cardiac tube. Because Rho GTPases, including Cdc42, are linked to the regulation of cell shape (Hall, 2012), we wanted to determine whether Cdc42 is also playing a subsequent role in DV lumen formation. To investigate whether interfering with Cdc42 function affects lumen formation, we examined *Hand-GAL4,UAS-GFP-moe;UAS-Cdc42^{N17}* embryos at stage 17, when embryogenesis is complete. As we showed previously (Fig. 3D–F) there are significant holes in the heart region of the DV that persist after embryonic DV morphogenesis is complete (Fig. 7 D-F). In these embryos, CB-CB contact is maintained by the Svp+ CBs, while the Tin+ CBs often remain unattached. We cross-sectioned *Hand-GAL4,UAS-GFP-moe;UAS-Cdc42^{N17}* embryos stained for GFP to label all CBs, and Wg to label the Svp+ CBs (see Materials and Methods) to examine lumen formation between both Tin+ and Svp+ CBs. We found that cross-sections taken through the heart where we observed Wg staining showed relatively normal lumen morphology (Fig. 7G–I). In contrast, sections taken through the heart, where there was an absence of Wg staining, showed severe defects in CB morphology and a failure to form a lumen (Fig. 7J–L). The latter results were not unexpected, because the Tin+ CBs fail to make contact with their contralateral partners, thus impeding lumen formation. However these results also demonstrate that loss of Cdc42 activity in the Svp+ CBs does not interfere with their ability to undergo the cell shape changes necessary for lumen formation. We further confirmed these findings by restricting expression of Cdc42^{N17} specifically in the Svp+ cells using the *Svp-GAL4* driver. In these embryos, staining with αSpectrin reveals that there are no significant defects in CB morphogenesis as observed in cross-section (Fig. 7N). From these results we conclude that that the primary function of Cdc42 during DV closure is to mediate the migration of the Tin + CBs to the dorsal midline and that the subsequent cell shape changes that the CBs undergo in order to form a lumen occur via an alternative mechanism.

Overexpression of dPAK does not rescue the dominant negative Cdc42 phenotype

Studies have shown that the Pak family of serine-theonine kinase proteins function as effectors for Cdc42 to regulate a diverse number of biological processes (Arias-Romero and Chernoff, 2008; Bokoch, 2003) and that dPak is required for *Drosophila* dorsal closure (Bahri et al., 2010; Conder et al., 2004). Because dPAK is also highly expressed in the DV (Harden et al., 1996), we examined *Pak* mutants during DV formation to determine if *Pak* functions downstream of *Cdc42* and mediates the DV defects observed in *Cdc42^{N17}* embryos. Because dominant negative expression of *Cdc42* results in DV abnormalities (Fig. 3D–F) and *Cdc42* activates *Pak*, we speculated that expression of membrane tethered form of *Pak* (*UAS-PAK-myr*) (Hing et al., 1999), which acts as a dominant gain-of-function protein, might rescue the phenotype observed in Cdc42 mutants. This strategy was used previously in *Drosophila* photoreceptor growth cones to rescue the phenotype of *dock*, which was shown to function upstream of dPak in axon guidance (Hing et al., 1999). Expression of *Pak-myr* in *Hand-GAL4, UAS-GFP-moe, UAS-Cdc42^{N17},UAS-Pak-myr* embryos failed to rescue the DV defects we observed in *Cdc42^{N17}* expressing embryos.

Specifically we still observed significant contact defects (data not shown) between *Tin*+ CBs in *Hand-GAL4, UAS-GFP-moe, UAS-Cdc42^{N17}, UAS-Pak-myr* embryos (74%; n=27) as compared to 82% (n=45) in *Hand-GAL4, UAS-GFP-moe, UAS-Cdc42^{N17}* embryos (82%; 37/45). Moreover, *Pak* LOF embryos (*Pak^{14} Pak3^{76A}*) were shown to maintain normal DV formation (Bahri et al., 2010). Taken together, these results suggest that *Cdc42* is acting independently of *Pak* during DV closure.

DISCUSSION

In this study we show for the first time a “buttoning” mechanism utilized by CBs during *Drosophila* DV closure. Specifically, we found that a genetically distinct subset of CBs, the Tin+ CBs, make contact at the dorsal midline with the opposing row prior to their neighbors (Fig. 1). Furthermore, we show that the cytoskeletal regulator Cdc42 is required specifically in the Tin+ CB leader cells to drive their forward migration to the embryonic midline ahead of their Svp+ neighbors. This mechanism is distinct from the zippering mechanism utilized by the DE cells during closure of the overlying epidermis. Our finding that specific subpopulations of CBs are predetermined to make initial contact with their opposing row is not limited to the *Drosophila* DV. A similar phenomenon has been described in chick embryos as “heart organizer” cells have been proposed to coordinate the cardiac fusion process, which in chick occurs bi-directionally from a central point of attachment (Moreno-Rodriguez et al., 2006).

Our results, with respect to the cellular mechanisms underlying DV closure, are of particular interest because both morphological and molecular studies have provided evidence for a close association between the DE and the CBs during their coordinated migration to the midline (Chartier et al., 2002; Haag et al., 1999). From our studies, we hypothesize that while the DE and the CBs may initially migrate to the dorsal midline in a coordinated fashion, the two cells types become selectively unattached as they approach the dorsal midline allowing for different patterns of cellular interactions. This idea is supported by our findings that in Cdc42 mutant embryos, the migration of the two CB rows from their lateral positions in the embryo to the dorsal region of the embryo is not impaired (Fig. 3). However, we do observe a loss of motility in Tin+ CBs during the final stages of migration to the dorsal midline. Thus, we propose that there are at least two distinct mechanisms that control CB migration, an early phase, which is independent of Cdc42, and a late phase that requires Cd42 in specific cardiac subtypes.

Why do the cells of the DE and the CBs undergo different morphogenetic behaviors to complete parallel tissue fusion processes? One possibility is that there are greater constraints on establishing and maintaining proper alignment between the two opposing CB rows during cardiac tube formation. The cells that make up the bilaterally symmetrical DV have highly specialized functions. For example, the Svp+ CBs undergo further morphogenetic changes to form the ostia or inflow tracts of the heart, while the Tin+ CBs are contractile and perform the pumping function. It is possible that the buttoning mechanism of DV closure may facilitate more accurate matching between bilateral CBs rows than zippering from both ends would allow.

The buttoning pattern of closure that we observe in the *Drosophila* DV depends upon a subset of CBs reaching the dorsal midline ahead of their adjacent neighbors. We propose that this is achieved via the differential regulation of cytoskeletal dynamics in a genetically distinct subset of CBs. In this study we show that Cdc42 activity is specifically required in the Tin+ pioneer cells in order for them to reach the dorsal midline. What accounts for the differential requirement for Cdc42 in the DV? It is possible that *cdc42* gene expression is tightly regulated in Tin+ CBs in the developing DV. This idea is consistent with recent studies that showed that Cdc42 is an indirect target of Tin in the adult fly heart where it plays an important role in regulating heart function (Qian et al., 2011). Alternatively, Cdc42 activity may be preferentially up regulated in the Tin+ cells or down regulated in the Svp+. However, our data showing that activated Cdc42 does not alter Svp+ CB migration argues against this latter possibility. Recent advancements in visualizing activation patterns of *Cdc42* in the heart tube (Kamiyama and Chiba, 2009) could prove to be an important tool for determining differential Cdc42 activity levels in the DV.

Interestingly, during *Drosophila* dorsal closure, Rac mutants have been shown to convert normal epithelial zippering to a pattern that more closely resembles the buttoning pattern we observe during wild type heart tube closure (Woolner et al., 2005). This abnormal pattern of epithelial closure is attributed to the presence of “protrusionless” stretches along the leading edge, supporting the idea that the differential regulation of the cytoskeleton can account for variations in morphogenetic behaviors during tissue fusion. Furthermore, recent studies show that epidermal closure differs between Tribolium and *Drosophila*. In contrast to zippering in *Drosophila*, Tribolium embryos utilize a “scalloped” approach (Panfilio et al., 2013), which also bears some resemblance to the buttoning mechanism we describe here. It will be of interest to determine whether differences in cytoskeletal regulation between the epidermal leading edge cells may also account for this morphogenetic behavior.

What are the upstream and downstream signaling pathways that result in the differential regulation of the cytoskeleton between Tin+ and Svp+ CBs? We show here that Cdc42 functions independently from dPak in DV formation, a known downstream target of Cdc42, suggesting that Cdc42 is functioning via an alternative mechanism in the DV. Further study of the proteins that regulate Cdc42 during DV closure should shed some light on how Rho GTPase activity can be modulated in different cell types during development.

Supplementary Material

Refer to Web version on PubMed Central for supplementary material.

Acknowledgments

We thank the Bloomington Stock Center for providing stocks and the Developmental Studies Hybridoma Bank for providing antibodies. We are also very grateful to Shreya Shah for her support on this project as well as Frank Macabenta for providing the illustrations. This work was supported by the Biomedical Science Education Postdoctoral Training Program Grant 5K12GM093854-05 and a National Science Foundation Grant (IOS-1123963) to S.G.K.

References

Abreu-Blanco MT, Verboon JM, Liu R, Watts JJ, Parkhurst SM. Drosophila embryos close epithelial wounds using a combination of cellular protrusions and an actomyosin purse string. J Cell Sci. 2012; 125:5984–5997. [PubMed: 23038780]

Abu-Issa R, Kirby ML. Heart field: from mesoderm to heart tube. Annu Rev Cell Dev Biol. 2007; 23:45–68. [PubMed: 17456019]

Arias-Romero LE, Chernoff J. A tale of two Paks. Biol Cell. 2008; 100:97–108. [PubMed: 18199048]

Bahri S, Wang S, Conder R, Choy J, Vlachos S, Dong K, Merino C, Sigrist S, Molnar C, Yang X, Manser E, Harden N. The leading edge during dorsal closure as a model for epithelial plasticity: Pak is required for recruitment of the Scribble complex and septate junction formation. Development. 2010; 137:2023–2032. [PubMed: 20501591]

Bokoch GM. Biology of the p21-activated kinases. Annu Rev Biochem. 2003; 72:743–781. [PubMed: 12676796]

Campos I, Geiger JA, Santos AC, Carlos V, Jacinto A. Genetic screen in Drosophila melanogaster uncovers a novel set of genes required for embryonic epithelial repair. Genetics. 2010; 184:129–140. [PubMed: 19884309]

Chartier A, Zaffran S, Astier M, Semeriva M, Gratecos D. Pericardin, a Drosophila type IV collagen-like protein is involved in the morphogenesis and maintenance of the heart epithelium during dorsal ectoderm closure. Development. 2002; 129:3241–3253. [PubMed: 12070098]

Chihara T, Kato K, Taniguchi M, Ng J, Hayashi S. Rac promotes epithelial cell rearrangement during tracheal tubulogenesis in Drosophila. Development. 2003; 130:1419–1428. [PubMed: 12588856]

Conder R, Yu H, Ricos M, Hing H, Chia W, Lim L, Harden N. dPak is required for integrity of the leading edge cytoskeleton during Drosophila dorsal closure but does not signal through the JNK cascade. Dev Biol. 2004; 276:378–390. [PubMed: 15581872]

Cripps RM, Olson EN. Control of cardiac development by an evolutionarily conserved transcriptional network. Dev Biol. 2002; 246:14–28. [PubMed: 12027431]

Crossley AC. The ultrastructure and function of pericardial cells and other nephrocytes in an insect: Calliphora erythrocephala. Tissue Cell. 1972; 4:529–560. [PubMed: 4348054]

Denholm B, Brown S, Ray RP, Ruiz-Gomez M, Skaer H, Hombria JC. crossveinless-c is a RhoGAP required for actin reorganisation during morphogenesis. Development. 2005; 132:2389–2400. [PubMed: 15843408]

Eaton S, Auvinen P, Luo L, Jan YN, Simons K. CDC42 and Rac1 control different actin-dependent processes in the Drosophila wing disc epithelium. J Cell Biol. 1995; 131:151–164. [PubMed: 7559772]

Edwards KA, Demsky M, Montague RA, Weymouth N, Kiehart DP. GFP-moesin illuminates actin cytoskeleton dynamics in living tissue and demonstrates cell shape changes during morphogenesis in Drosophila. Dev Biol. 1997; 191:103–117. [PubMed: 9356175]

Etienne-Manneville S, Hall A. Rho GTPases in cell biology. Nature. 2002; 420:629–635. [PubMed: 12478284]

Fox DT, Homem CC, Myster SH, Wang F, Bain EE, Peifer M. Rho1 regulates Drosophila adherens junctions independently of p120ctn. Development. 2005; 132:4819–4831. [PubMed: 16207756]

Gajewski K, Choi CY, Kim Y, Schulz RA. Genetically distinct cardial cells within the Drosophila heart. Genesis. 2000; 28:36–43. [PubMed: 11020715]

Gates J, Mahaffey JP, Rogers SL, Emerson M, Rogers EM, Sottile SL, Van Vactor D, Gertler FB, Peifer M. Enabled plays key roles in embryonic epithelial morphogenesis in Drosophila. Development. 2007; 134:2027–2039. [PubMed: 17507404]

Haag TA, Haag NP, Lekven AC, Hartenstein V. The role of cell adhesion molecules in Drosophila heart morphogenesis: faint sausage, shotgun/DE-cadherin, and laminin A are required for discrete stages in heart development. Dev Biol. 1999; 208:56–69. [PubMed: 10075841]

Hall A. Rho family GTPases. Biochem Soc Trans. 2012; 40:1378–1382. [PubMed: 23176484]

Han Z, Yi P, Li X, Olson EN. Hand, an evolutionarily conserved bHLH transcription factor required for Drosophila cardiogenesis and hematopoiesis. Development. 2006; 133:1175–1182. [PubMed: 16467358]

Harden N, Lee J, Loh HY, Ong YM, Tan I, Leung T, Manser E, Lim L. A Drosophila homolog of the Rac- and Cdc42-activated serine/threonine kinase PAK is a potential focal adhesion and focal complex protein that colocalizes with dynamic actin structures. Mol Cell Biol. 1996; 16:1896–1908. [PubMed: 8628256]

Harden N, Loh HY, Chia W, Lim L. A dominant inhibitory version of the small GTP-binding protein Rac disrupts cytoskeletal structures and inhibits developmental cell shape changes in Drosophila. Development. 1995; 121:903–914. [PubMed: 7720592]

Harden N, Ricos M, Ong YM, Chia W, Lim L. Participation of small GTPases in dorsal closure of the Drosophila embryo: distinct roles for Rho subfamily proteins in epithelial morphogenesis. J Cell Sci. 1999; 112(Pt 3):273–284. [PubMed: 9885281]

Hing H, Xiao J, Harden N, Lim L, Zipursky SL. Pak functions downstream of Dock to regulate photoreceptor axon guidance in Drosophila. Cell. 1999; 97:853–863. [PubMed: 10399914]

Jacinto A, Wood W, Balayo T, Turmaine M, Martinez-Arias A, Martin P. Dynamic actin-based epithelial adhesion and cell matching during Drosophila dorsal closure. Curr Biol. 2000; 10:1420–1426. [PubMed: 11102803]

Johndrow JE, Magie CR, Parkhurst SM. Rho GTPase function in flies: insights from a developmental and organismal perspective. Biochem Cell Biol. 2004; 82:643–657. [PubMed: 15674432]

Kamiyama D, Chiba A. Endogenous activation patterns of Cdc42 GTPase within Drosophila embryos. Science. 2009; 324:1338–1340. [PubMed: 19498173]

Kawahara A, Nishi T, Hisano Y, Fukui H, Yamaguchi A, Mochizuki N. The sphingolipid transporter spns2 functions in migration of zebrafish myocardial precursors. Science. 2009; 323:524–527. [PubMed: 19074308]

Lo PC, Skeath JB, Gajewski K, Schulz RA, Frasch M. Homeotic genes autonomously specify the anteroposterior subdivision of the Drosophila dorsal vessel into aorta and heart. Dev Biol. 2002; 251:307–319. [PubMed: 12435360]

Lu Y, Settleman J. The Drosophila Pkn protein kinase is a Rho/Rac effector target required for dorsal closure during embryogenesis. Genes Dev. 1999; 13:1168–1180. [PubMed: 10323867]

Macabenta FD, Jensen AG, Cheng YS, Kramer JJ, Kramer SG. Frazzled/DCC facilitates cardiac cell outgrowth and attachment during Drosophila dorsal vessel formation. Dev Biol. 2013

Magie CR, Meyer MR, Gorsuch MS, Parkhurst SM. Mutations in the Rho1 small GTPase disrupt morphogenesis and segmentation during early Drosophila development. Development. 1999; 126:5353–5364. [PubMed: 10556060]

Martin P, Wood W. Epithelial fusions in the embryo. Curr Opin Cell Biol. 2002; 14:569–574. [PubMed: 12231351]

Medioni C, Astier M, Zmojdzian M, Jagla K, Semeriva M. Genetic control of cell morphogenesis during Drosophila melanogaster cardiac tube formation. J Cell Biol. 2008; 182:249–261. [PubMed: 18663140]

Medioni C, Senatore S, Salmand PA, Lalevee N, Perrin L, Semeriva M. The fabulous destiny of the Drosophila heart. Curr Opin Genet Dev. 2009; 19:518–525. [PubMed: 19717296]

Millard TH, Martin P. Dynamic analysis of filopodial interactions during the zippering phase of Drosophila dorsal closure. Development. 2008; 135:621–626. [PubMed: 18184725]

Molina MR, Cripps RM. Ostia, the inflow tracts of the Drosophila heart, develop from a genetically distinct subset of cardial cells. Mech Dev. 2001; 109:51–59. [PubMed: 11677052]

Moreno-Rodriguez RA, Krug EL, Reyes L, Villavicencio L, Mjaatvedt CH, Markwald RR. Bidirectional fusion of the heart-forming fields in the developing chick embryo. Dev Dyn. 2006; 235:191–202. [PubMed: 16252277]

Nobes CD, Hall A. Rho, rac, and cdc42 GTPases regulate the assembly of multimolecular focal complexes associated with actin stress fibers, lamellipodia, and filopodia. Cell. 1995; 81:53–62. [PubMed: 7536630]

Panfilio KA, Oberhofer G, Roth S. High plasticity in epithelial morphogenesis during insect dorsal closure. Biol Open. 2013; 2:1108–1118. [PubMed: 24244847]

Pirraglia C, Jattani R, Myat MM. Rac function in epithelial tube morphogenesis. Dev Biol. 2006; 290:435–446. [PubMed: 16412417]

Qian L, Wythe JD, Liu J, Cartry J, Vogler G, Mohapatra B, Otway RT, Huang Y, King IN, Maillet M, Zheng Y, Crawley T, Taghli-Lamallem O, Semsarian C, Dunwoodie S, Winlaw D, Harvey RP, Fatkin D, Towbin JA, Molkentin JD, Srivastava D, Ocorr K, Bruneau BG, Bodmer R. Tinman/Nkx2-5 acts via miR-1 and upstream of Cdc42 to regulate heart function across species. J Cell Biol. 2011; 193:1181–1196. [PubMed: 21690310]

Santiago-Martinez E, Soplop NH, Patel R, Kramer SG. Repulsion by Slit and Roundabout prevents Shotgun/E-cadherin-mediated cell adhesion during Drosophila heart tube lumen formation. J Cell Biol. 2008; 182:241–248. [PubMed: 18663139]

Sellin J, Albrecht S, Kolsch V, Paululat A. Dynamics of heart differentiation, visualized utilizing heart enhancer elements of the Drosophila melanogaster bHLH transcription factor Hand. Gene Expr Patterns. 2006; 6:360–375. [PubMed: 16455308]

Tao Y, Schulz RA. Heart development in Drosophila. Semin Cell Dev Biol. 2007; 18:3–15. [PubMed: 17208472]

Togel M, Pass G, Paululat A. The Drosophila wing hearts originate from pericardial cells and are essential for wing maturation. Dev Biol. 2008; 318:29–37. [PubMed: 18430414]

Totong R, Schell T, Lescroart F, Ryckebusch L, Lin YF, Zygmunt T, Herwig L, Krudewig A, Gershoony D, Belting HG, Affolter M, Torres-Vazquez J, Yelon D. The novel transmembrane protein Tmem2 is essential for coordination of myocardial and endocardial morphogenesis. Development. 2011; 138:4199–4205. [PubMed: 21896630]

Trinh LA, Stainier DY. Fibronectin regulates epithelial organization during myocardial migration in zebrafish. Dev Cell. 2004; 6:371–382. [PubMed: 15030760]

Van Aelst L, Symons M. Role of Rho family GTPases in epithelial morphogenesis. Genes Dev. 2002; 16:1032–1054. [PubMed: 12000787]

Warner SJ, Longmore GD. Distinct functions for Rho1 in maintaining adherens junctions and apical tension in remodeling epithelia. J Cell Biol. 2009; 185:1111–1125. [PubMed: 19506041]

Wood W, Jacinto A, Grose R, Woolner S, Gale J, Wilson C, Martin P. Wound healing recapitulates morphogenesis in Drosophila embryos. Nat Cell Biol. 2002; 4:907–912. [PubMed: 12402048]

Woolner S, Jacinto A, Martin P. The small GTPase Rac plays multiple roles in epithelial sheet fusion–dynamic studies of Drosophila dorsal closure. Dev Biol. 2005; 282:163–173. [PubMed: 15936337]

Highlights

- Heart closure occurs via a buttoning pattern distinct from epithelial zippering.
- A subset of cardiac cells makes initial contact at the dorsal midline.
- Cdc42 is required in cardiac leader cells for their dorsal migration.
- Inhibition of Cdc42 in cardiac leader cells leads to loss of protrusions.
- Non-leader cells are insensitive to Cdc42 inhibition.

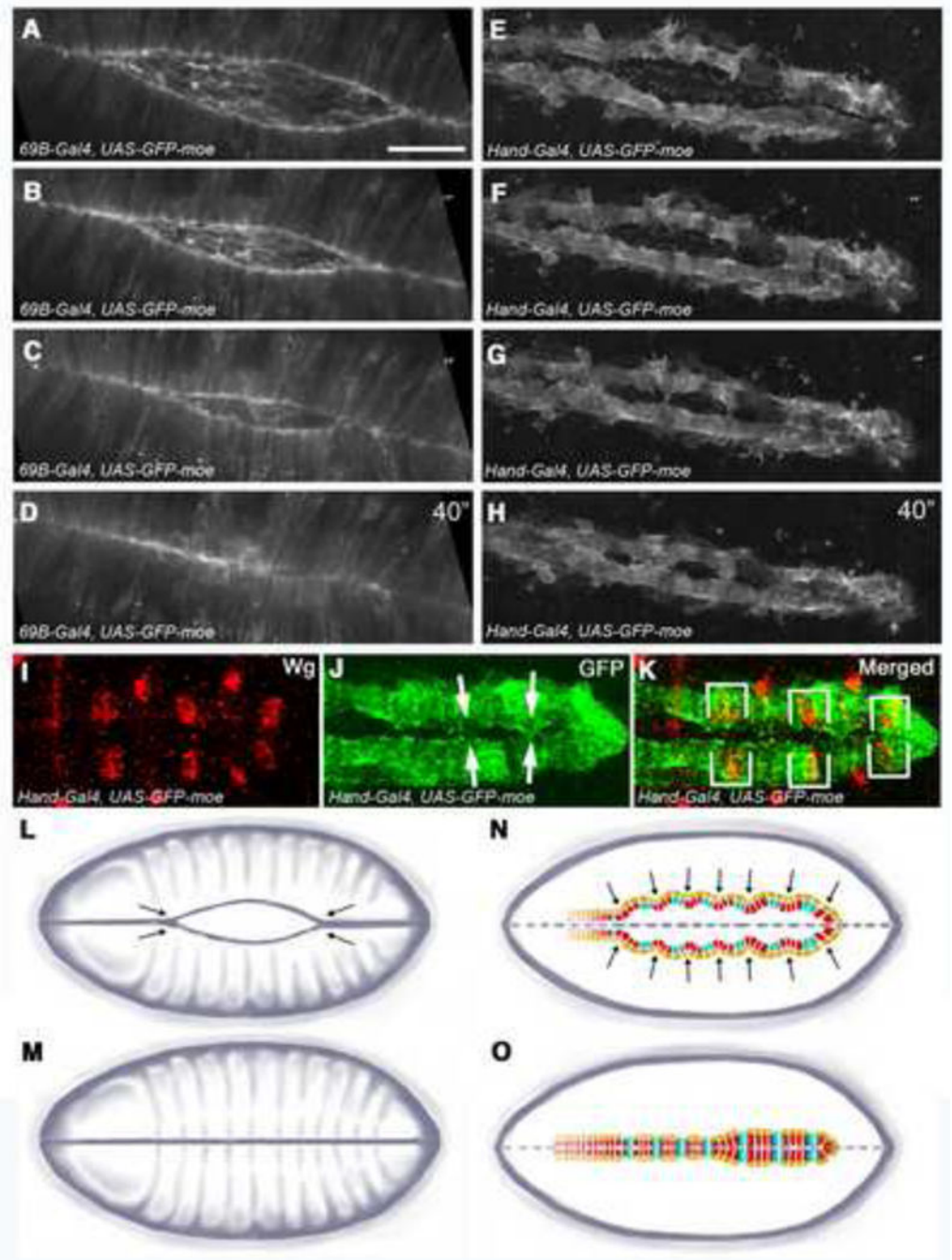

Figure 1. Comparison between the cellular mechanisms underlying dorsal closure and DV closure

(A-D) Movie stills showing embryos expressing GFP-moe in the dorsal epithelium using *69B-GAL4*. Still frames were taken from a movie capturing 40 minutes of dorsal closure, illustrating the zippering mechanism by which the dorsal ectoderm closes. See Movie S1 in the supplementary material. Time is in minutes. (E-H) Movie stills showing embryos expressing GFP-moe in the DV using *Hand-GAL4* showing that DV closure occurs at multiple independent points along the A-P axis of the embryo in a “buttoning” pattern, divergent from the zippering mechanism for dorsal closure. See Movie S2 in the

supplementary material. (I-K) *Hand-GAL4; UAS-GFP-moe* embryos stained with anti-Wingless (Wg) to identify *Svp*+ CB (I) and anti-GFP to label the DV. The CBs that most often make initial contact (arrows) with their contralateral partners are negative for Wg and thus are Tin+ CBs. (K) Brackets show *Svp*+ CB stained with anti-Wingless are further apart from their partners than neighboring CBs. (L-O) Schematic illustrating how the dorsal ectoderm closes via zippering (L,M) compared with the “buttoning” effect seen in the developing DV (N,O). In (N,O) Tin+ CBs are shown in red, *Svp*+ CBs are blue and pericardial cells are tan. Tin+ CBs act as pioneer cardiac cells, making contact with their partnering CB before Svp+ CBs in 72% (n=18) of embryos. Scale bar is 40um.

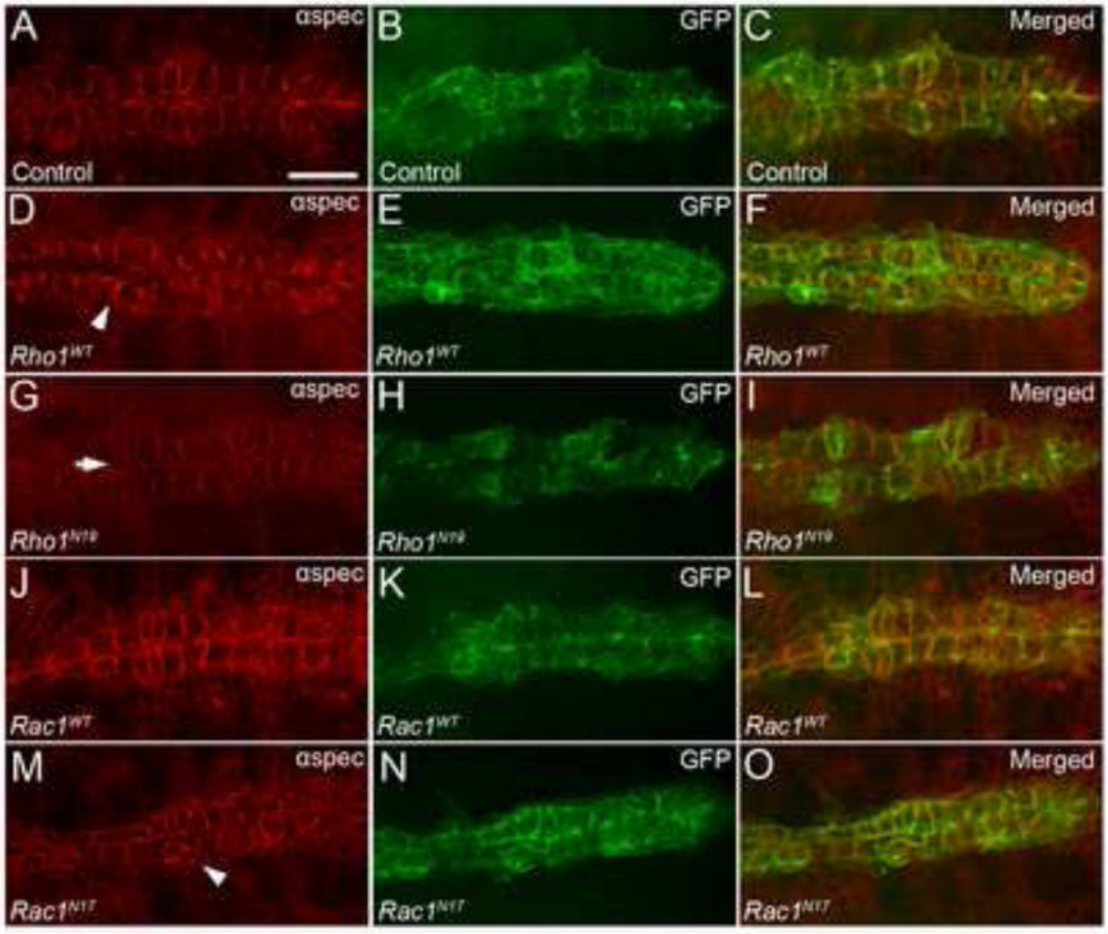

Figure 2. Dysregulation of *Rho* and *Rac* GTPases in the DV

(A-C) Control (yw; *Hand-GAL4, UAS-GFP-moe*) embryos at stage 17 stained with anti-αSpectrin, which labels CB lateral and luminal membranes (A) and anti-GFP (B) in the heart region of the DV. Merged image is shown in (C). (D-O) Stage 17 embryos overexpressing wild type or dominant negative Rho1 or Rac1 in the *Hand-GAL4, UAS-GFP-moe* background and stained with anti-αSpectrin (D,G,J,M) and anti-GFP (E,H,K,N) in the heart region of the DV. (D) *Rho1* overexpressing embryos appear to show stronger accumulation of αSpectrin at CB lateral membranes (arrowhead) as compared with wild type (A). (G-I) Overexpression of dominant negative *Rho1* (*Rho1*^{N19}) results in small holes (arrow) between *Svp+* CBs, which can be identified by their elongated shape relative to the Tin+ CBs. (J-L) *Rac1*^{WT} overexpressing embryos appear indistinguishable from wild type and overexpression of dominant negative *Rac1* (*Rac1*^{N17}) (M-O) produces in minor defects in CB positioning (arrowhead) (M) in the DV. See Table 1 for quantitative data. Scale bar is 20um.

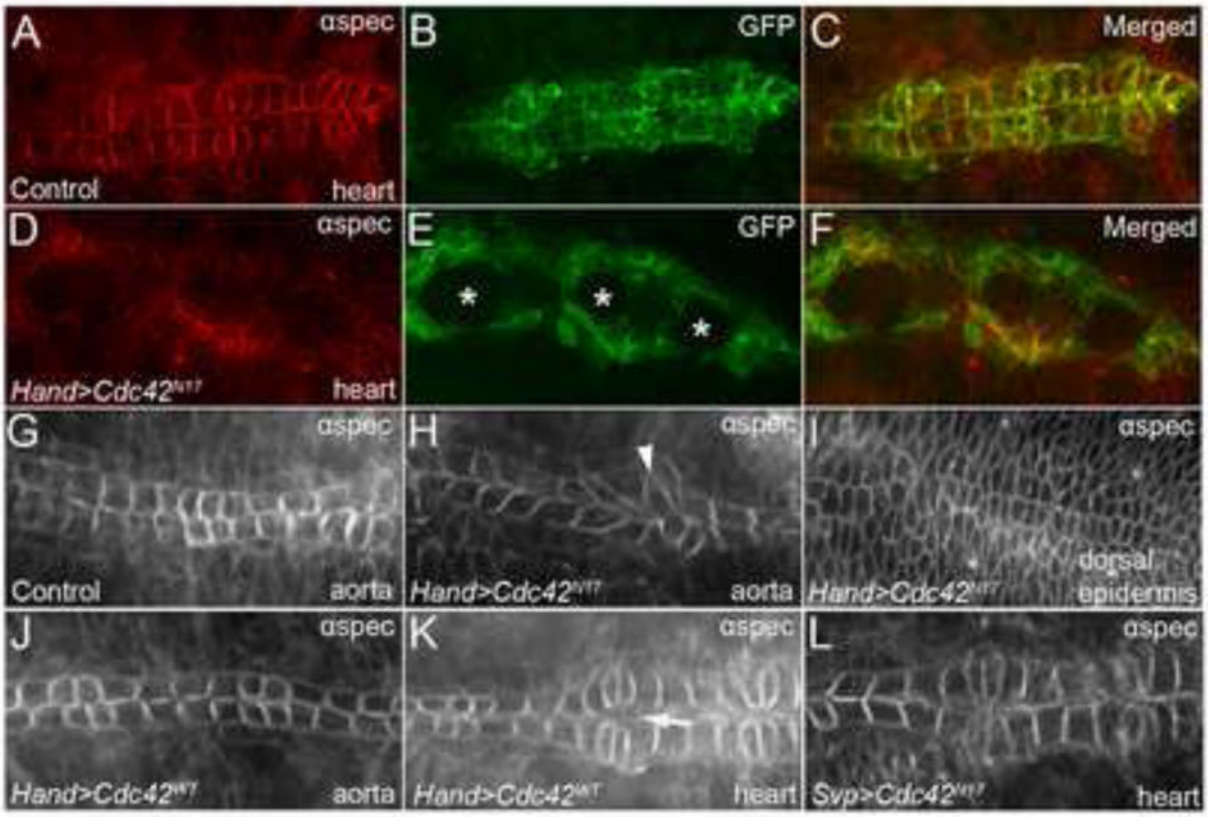

Figure 3. Dominant negative expression of Cdc42 causes severe DV defects

(A-C) Stage 17 *Hand-GAL4,UAS-GFP-moe* (control) embryos in whole mount stained with anti-αSpectrin (A) and anti-GFP (B) in the heart region of the DV to show normal CB morphology and alignment at the dorsal midline. (C) is a merged image of (A) and (B). Overexpression of dominant negative *Cdc42 (Cdc42 ^{N17})* (D-F) in the DV produces large holes (asterisks) within the heart. Anti-αSpectrin staining of the aorta (G-H) reveals abnormal CB morphology (arrowhead) in *Cdc42^{N17}* mutants (H) compared to wild type (*w^{1118}*) aortas (G), albeit no CB contact defects as seen in the heart region (E). (I) *Cdc42^{N17}* mutants maintain proper dorsal ectodermal closure, evident by anti-αSpectrin staining. (I) is the same embryo as shown in (D-F) at a different focal plane. (J-K) Overexpression of wild type *Cdc42* (*Cdc42^{WT}*) does not cause any defects in the aorta (J) and results in only minor gaps (arrow) between *Svp+* cells in the heart (K). (L) Overexpression of *Cdc42^{N17}* specifically in Svp+ CBs with *Svp-GAL4* results in normal DV closure and CB morphology as apparent by anti-αSpectrin staining. See Table 1 for quantitative data.

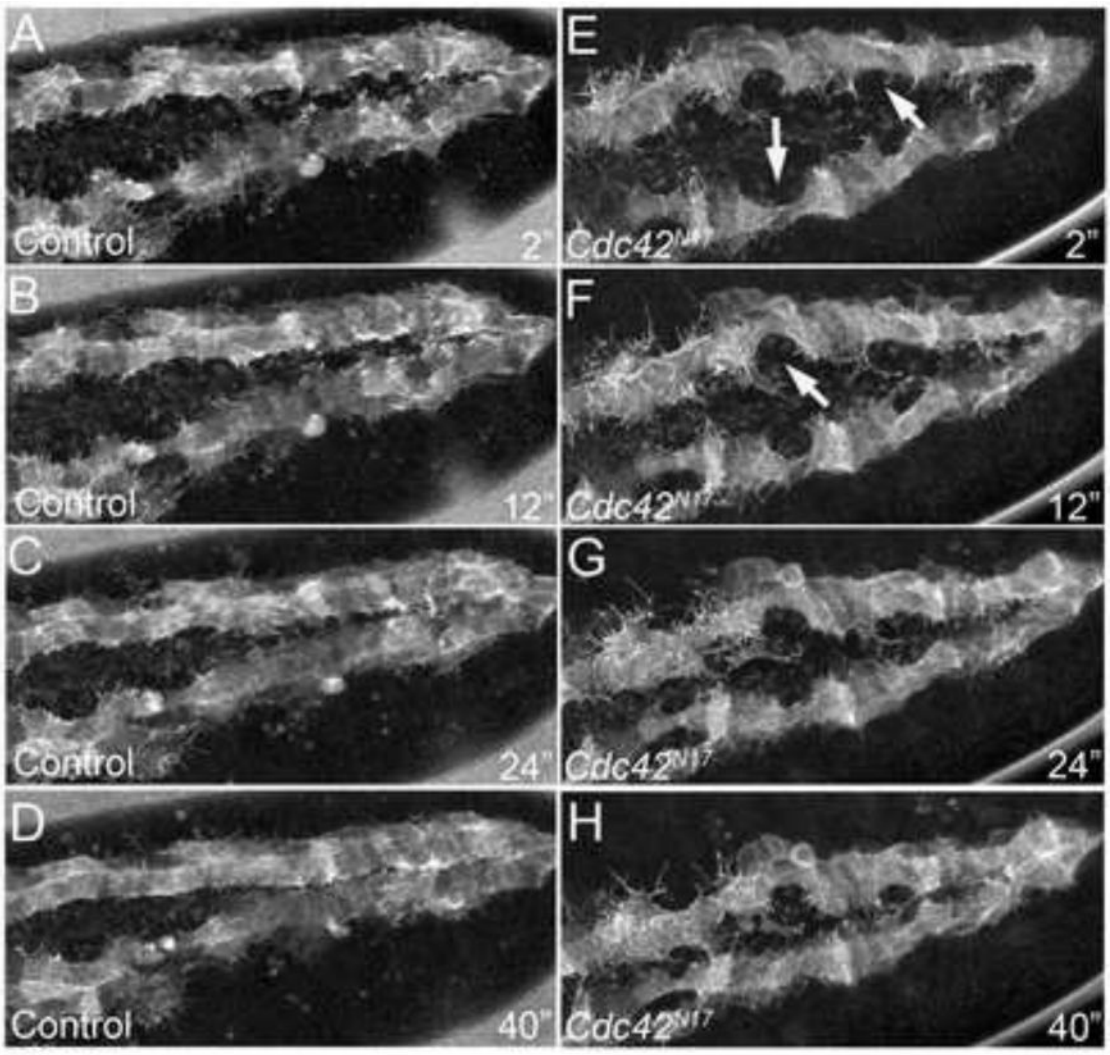

Figure 4. *Cdc42*^{N17} mutants have defects in cell migration during DV formation

Movie stills showing embryos expressing *GFP-moe* in the DV using *Hand-GAL4*. Control (*Hand-GAL4, UAS-GFP-moe)* (A-D) and *Cdc42*^{N17} mutant (*Hand-GAL4, UAS-GFP-moe;UAS-Cdc42*^{N17}*)* (E-H) movie stills sequential still frames taken from live developing whole mount embryos beginning at stage 15. (E-H) Regions (arrows) of *Cdc42*^{N17}mutant DVs show decreased motility and reduced filopodial number. Time is in minutes. Images extracted from Movies S3 and S4 in the Supplemental Material.

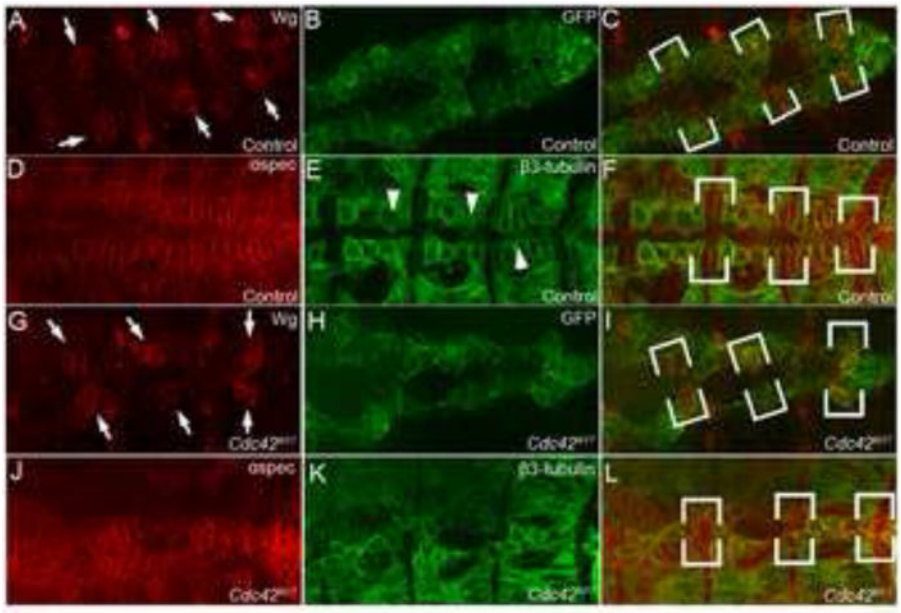

Fig. 5. Svp+ CBs make contact with their contralateral partner before *Tin*+ CBs in *Cdc42*^{N17} mutants

(A-F) Representative images of a wild type (*Hand-GAL4,UAS-GFP-moe)* embryos labeled with anti-Wingless (*Wg*) (A) which labels six pairs of *seven-up (Svp+)* CBs (arrows) and anti-GFP (B) to visual CB membranes. Co-immunofluorescence staining of anti-αSpectrin (D) and anti-®3-tubulin staining (E) of Control embryos to visualize cell membranes and Tin+ CBs respectively. (G-L) Representative images of a *Cdc42* mutant (*Hand-GAL4,UAS-GFP-moe;* UAS-*Cdc42*^{N17}*)* embryo co-labeled with anti-*Wg* (G), anti-GFP (H), anti-αSpectrin (J) and anti-β3-tubulin (K). In the wild type heart region (C and F), contralateral Svp+ CBs (brackets) are normally further apart from their contralateral than adjacent Tin+ CBs (arrowheads), which make initial contact at the dorsal midline (E). (I and L) In *Cdc42*^{N17} mutants, the Svp+ CBs (brackets) are closer to their contralateral partners as compared to Tin+ CBs. C, F, I, and L are merged images of A&B, D&E, G&H, J&K respectively.

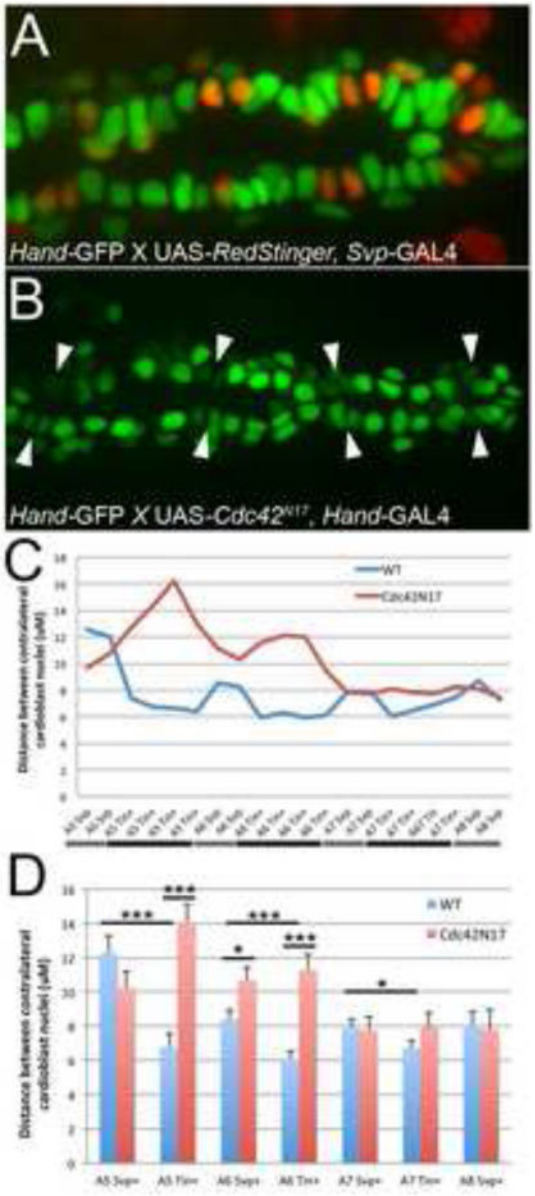

Figure 6. Tin+ CBs normally guide DV closure but are impaired when expressing *Cdc42^{N17}*

(A) Representative image of a live wild type (UAS-*Redstinger*; *Svp*-GAL4, *Hand*-GFP) embryo. Svp+ CBs are labeled in red, and Tin+ CBs in green. (B) Representative image of a live *Cdc42^{N17}* mutant (UAS-*Cdc42^{N17}*, *Hand*-GAL4; *Hand*-GFP) embryo. Svp+ CBs (arrowheads) were identified by cellular morphology and counting CB number from the posterior end of the embryo. Wild type (WT) Tin+ CBs (green) are closer to their contralateral partners than Svp+ CBs (red) (A). Conversely, Tin+ CBs of *Cdc42^{N17}* mutants appear further away from their contralateral partners than Svp+ CBs (B). (C, D) Quantification of distance measurements taken between contralateral CB nuclei (μM) in WT and *Cdc42^{N17}* mutants between abdominal segments A5–A8. In control hearts, note the significant decrease in distance between *Tin*+ CB nuclei pairs compared to *Svp*+ CB nuclei pairs in segments A5-A7 (D). This data suggests Tin+ CBs are closer together migrate ahead

of the Svp+ CBs. Interestingly, quantification of nuclei distance in *Cdc42*^{N17} mutants demonstrates that Tin+ CBs are now further away from their contralateral partners in segments A5 and A6 of the DV (C-D). It should also be noted that the distance between Svp + CBs within A6 of *Cdc42*^{N17} hearts were also significantly different than wild type. This finding could be a result of motile deficient neighboring Tin+ CBs anchoring Svp+ CBs and slowing their migration. 3 sets of measurements were recorded during DV closure for each embryo (WT n=7; *Cdc42*^{N17}mutants n=6). SE bars are displayed. * P<0.05, ** P<0.01, *** P<0.001.

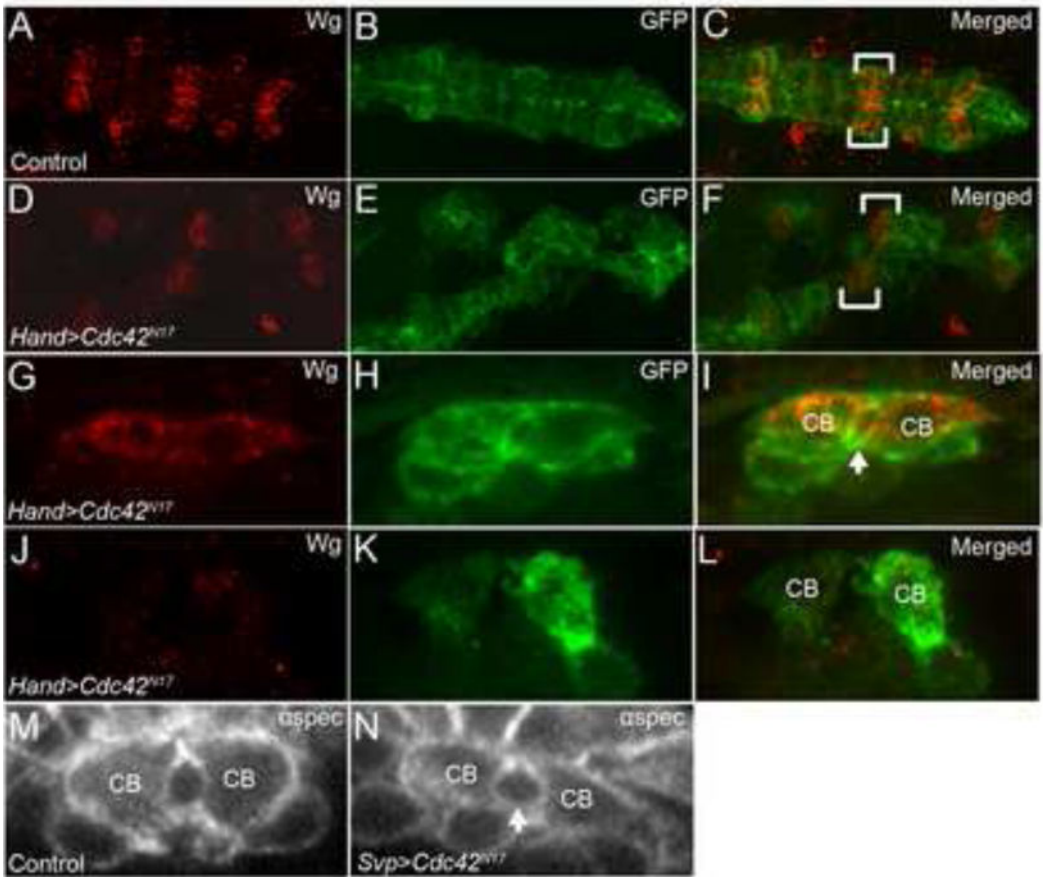

Figure 7. Cdc42 activity is required in Tin+ CBs but not Svp+ CBs during DV closure

(A-C) *Hand-GAL4,UAS-GFP-Moe* (wild type) embryos in whole mount, stained with anti-Wingless *(Wg)* (A, red) to label the Svp+ CBs and anti-GFP (B, green) in the heart region of the DV. At stage 17 in the wild type heart, six pairs of Wg-expressing CBs come together to form *seven-up*$^{+}$ (*Svp+*) ostia cells. (C) is a merge of A and B. Brackets show positions of Wg expressing CBs. (D-F) In *Cdc42*^{N17}mutants, strong defects in DV closure are observed. Brackets show Wg-expressing CBs in merged image (F). (G-L) Cross-sections taken through the heart region of the DV in embryos expressing *Cdc42*^{N17} in all CBs with Hand-GAL4 that were immunostained with anti-Wg (G,J) and anti-GFP (H,K). Svp+ CBs that label with Wg (G) are able to form a heart lumen (arrow in merge image, I), while Tin+ CBs, negative for *Wg*, (J) show a no lumen phenotype (merged image, L). Overexpression of *Cdc42*^{N17}specifically in Svp+ CBs with *Svp-GAL4* results in normal CB morphology and lumen formation (arrow, N) in cross-section as apparent by anti-αSpectrin staining as compared to control embryos (M).

Table 1

Quantification of DV phenotypes in whole mount embryos.

Genotype	Defect in *Tin*+ CB− CB Contact	Defect in only *Svp*+ CB− CB Contact
WT	0% (0/19)	16% (3/19)
UAS-Rho1^{WT} x Hand-Gal4	0% (0/17)	18% (3/17)
UAS-Rho1^{N19} x Hand-Gal4	0% (0/14)	57% (8/14)§
UAS-Rac1^{WT} x Hand-Gal4	0% (0/14)	14% (2/14)
UAS-Rac1^{N17} x Hand-Gal4	0% (0/18)	22% (4/18)
UAS-Cdc42^{N17} x Hand-Gal4	82% (37/45)§	6% (2/45)
UAS-Cdc42^{WT} x Hand-Gal4	0% (0/23)	35% (8/23)
UAS-Cdc42^{V12} x Hand-Gal4	0% (0/12)	17% (2/12)
UAS-Cdc42^{N17} x Svp-Gal4	0% (0/51)	18% (9/51)
UAS-Cdc42^{N17} x Prc-Gal4	0% (0/15)	20% (3/15)

§Data sets differ significantly from WT with a P value of <0.05 by the T-test.